Pergamon

Int. J. Heat Mass Transfer. Vol. 38, No. 8, pp. 1397–1407, 1995

0017-9310/95 $9.50+0.00

0017-9310(94)00267-3

Natural convection and conduction in inclined enclosures bounded by a wall with honeycomb structure

E. K. LAKHAL
Faculty of Science, Semlalia, B.P. S-15, Marrakesh, Morocco

and

E. BILGEN† and P. VASSEUR
Ecole Polytechnique Box 6079, 'City Center', Montreal, Pc, Canada H3C 3A7

(*Received* 18 *April* 1994 *and in final form* 29 *July* 1994)

Abstract—The natural convection and conduction heat transfer in inclined rectangular enclosures with honeycomb structure attached to the heated wall is numerically studied. The boundary conditions were constant heat flux on the wall and fins, isothermal on the bounding long sides and adiabatic on the short sides. The governing parameters are the Rayleigh number ($10^4 \leqslant Ra \leqslant 10^8$), the aspect ratio of the enclosures ($2.5 \leqslant A = H'/L' \leqslant 10$), the dimensionless lengths of the partitions ($0 \leqslant B = l'/L'_1 \leqslant 1$), the aspect ratio of the micro-cavities ($0.25 \leqslant C = h'/L' \leqslant 2.5$), the inclination angle ($5 \leqslant \phi \leqslant 90°$), the wall thickness ($0 \leqslant w = w'/L' \leqslant 1$). The fin thickness was ($e = e'/H' = 0.08$). The Prandtl number was constant ($Pr = 0.72$) and the conductivity ratio varied as ($10^{-3} \leqslant k_r \leqslant 10^5$). Local and average Nusselt numbers along the long sides are calculated as a function of various parameters. Streamlines and isotherms are produced.

INTRODUCTION

Honeycomb structures are often used in various applications to modify heat transfer. As a result, a tall enclosure is formed, vertical or inclined, containing a two-dimensional honeycomb structure. In two-dimensional cases, the system has two active long sides, one of which is with finite thickness and conductivity and equipped with conducting fins, and two connecting short sides, which are insulated. Depending on the size of the fins, equidistant open micro-cavities are formed that are connected to each other by the channel formed in the tall enclosure.

A review of the literature shows that there are various studies on heat transfer in cavities containing fins similar to that described here. For building elements with passive utilization of solar energy, a theoretical study reported on a two-dimensional honeycomb structure where conduction heat and mass transfers were assumed to be negligible [1]. The effect of natural convection in a micro-cavity of a system induced by radiation was reported later for dimensionless micro-cavity height from 0.2 to 1 and with isothermal active walls [2]. It was shown that heat transfer by natural convection decreased with decreasing aspect ratio, with increasing radiation and radiation incidence angle.

Vertical rectangular enclosures with adiabatic fins attached to the isothermal heated wall opposing an isothermal cold wall were studied numerically [3]. The enclosure aspect ratio was from 2 to 3, the dimensionless fin length from 0 to 0.75, micro-cavity height from 0.30 to 0.67. Their study showed that the heat transfer through the cold wall was reduced with respect to the case without fins and this reduction was enhanced with increasing fin length and decreasing Rayleigh number. In a subsequent work [4], this study was extended to an inclined tall enclosure case with the enclosure aspect ratio from 2.5 to ∞, dimensionless fin length from 0 to 1, micro-cavity height from 0.25 to 2. The Rayleigh number was from 10^4 to 2×10^5. They found that fin length was an important parameter: at low Rayleigh numbers, the heat transfer was reduced with increasing fin length but at high Rayleigh numbers there was an optimum value. Heat transfer was reduced for decreasing micro-cavity height and passed from a maximum for an inclination angle. They also showed that the problem in tall cavities with an infinite number of fins could be solved similarly to that in a single micro-cavity using the periodicity hypothesis. The results of these studies would be applicable to problems where fins were made from non-conducting materials such as plastics, but not to those made from construction materials such as concrete and brick.

Starting from a different premise, Scozia and Frederick [5] numerically studied two-dimensional

† Author to whom correspondence should be addressed.

NOMENCLATURE

A	aspect ratio, H'/L'
a	dimensionless distance in the enclosure, x'/L'_1
B	dimensionless fin length, l'/L'_1
C	dimensionless micro-cavity height, h'/L'
e	dimensionless fin thickness, e'/H'
e'	fin thickness
g	acceleration due to gravity [m s^{-2}]
h'	height of the micro-cavity [m]
h	local heat transfer coefficient [W m^{-2} K^{-1}]
$\bar{h}$	average heat transfer coefficient on heated wall [W m^{-2} K^{-1}]
H'	total height of calculation domain [m]
k	thermal conductivity [W m^{-1} K^{-1}]
k_r	thermal conductivity ratio, k_s/k_f
l'	fin length [m]
L'	total width of calculation domain [m]
L'_1	width of the enclosure with fins [m]
Nu	mean Nusselt number, $\bar{h}L'/k_f$
Nu_0	mean Nusselt number of the bench mark problem
n	number of micro-cavities, A/C
N	number of fins, $n-1$
p	dimensionless pressure, $p = \dfrac{p' + \rho_f g(y' \sin\phi - x' \cos\phi)}{\rho_f(\alpha_f/L')^2}$
p'	pressure [Pa]
Pr	Prandtl number, ν_f/α_f
q	heat flux [W m^{-2}]
Ra	Rayleigh number, $(g\beta qL'^4)/(k_f\nu_f\alpha_f)$
T	dimensionless temperature, $(T'-T'_2)/\Delta T'$
T'	solid wall temperature [K]
ΔT	temperature difference, $T'_1 - T'_2$ [K]
$\Delta T'$	temperature difference, qL'/k_f [K]
u, v	dimensionless velocity in x and y direction, $(u', v')/(\alpha_f/L')$
u', v'	velocities in x' and y' directions [m s^{-1}]
w	dimensionless wall width, w'/L'
x, y	dimensionless Cartesian coordinates, $(x', y')/L'$
x', y'	Cartesian coordinates.

Greek symbols

α	thermal diffusivity [m^2 s^{-1}]
β	volumetric coefficient of thermal expansion [K^{-1}]
ν	kinematic viscosity [m^2 s^{-1}]
ρ	fluid density [kg·m^{-3}]
ϕ	tilt angle [°]
Ψ	dimensionless stream function, Ψ'/α_f.

Subscripts

1	left boundary
2	right boundary
ext	extremum
f	fluid
loc	local
max	maximum
s	solid.

Superscript

$'$	dimensional variables.

flow of air in a differentially heated slender enclosure with conducting fins attached on the cold wall. The enclosure aspect ratio was varied from 20 to ∞, that of micro-cavities from 2.5 to 20 and the Rayleigh number from 10^3 to 10^5. They studied the effect of the micro-cavity aspect ratio of the flow and temperature fields, and derived useful guidelines for collector and cover design when the fins could be attached to the cold wall: however, they could not be attached to the heated wall, as in the case with Trombe walls and electronic components.

In a recent investigation [6], the problem with perfectly conducting fins was numerically studied. It was found that the heat transfer through the cold wall could be reduced considerably by using conducting fins attached to the heated wall. The heat transfer was dominated by conduction when the dimensionless fin length was about 0.77 and the dimensionless micro-cavity aspect ratio about 0.3. This effect was enhanced with inclination angle.

It is seen that earlier studies are mostly concerned with natural convection in enclosures with fins attached to one of the long sides, which are rigid walls with zero thickness subjected to various boundary conditions. That is, the thickness and conduction in the bounding wall containing the fins are not considered. Yet, in many applications, the bounding wall with fins has a finite thickness and conductivity, which affects the natural convection in the enclosure.

The purpose of the present investigation is to study heat transfer by natural convection and conduction in enclosures containing a honeycomb structure attached to a wall. Of the two active long sides, one is with finite thickness and conductivity and equipped with conducting fins, and the other is kept at constant temperature. Two connecting short sides are insulated. As the application varies from cooling of electronic components to passive solar collectors with massive heated walls, the effects of various geometrical parameters (enclosure aspect ratio, A, fin

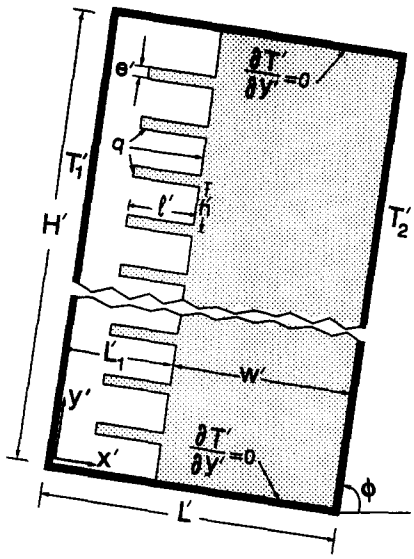

Fig. 1. Schematic of the problem, boundary conditions and the coordinate system.

length, B, micro-cavity aspect ratio, C and inclination angle, ϕ) on the heat transfer are investigated for practical ranges of Ra with Pr maintained at 0.72 (air).

PROBLEM DESCRIPTION

A schematic of the system with geometrical and boundary conditions is shown in Fig. 1. Heat is released by a constant flux from the inside surface of the wall with finite thickness and that of the fins, and is transferred by convection and conduction through the left long side at T'_1 and by conduction through the right at T'_2. For each aspect ratio, the number n of micro-cavities varies with C, with the number N of the fins following the relation $n = A/C = N+1$. The dimensionless fin thickness, e, and length, B, are attached to the massive wall at equal distance h' from each other. It is assumed that the third dimension of the enclosure is large enough and the flow can be considered two-dimensional. It is also assumed that the Boussinesq approximation applies.

MATHEMATICAL MODELLING

Using non-dimensional variables defined in the nomenclature, the non-dimensional governing equations are obtained as

$$\frac{\partial u}{\partial x}+\frac{\partial v}{\partial y}=0 \tag{1}$$

$$u\frac{\partial u}{\partial x}+v\frac{\partial u}{\partial y}=-\frac{\partial p}{\partial x}+\Gamma\nabla^2 u-\frac{Ra}{Pr}T\cos\phi \tag{2}$$

$$u\frac{\partial v}{\partial x}+v\frac{\partial v}{\partial y}=-\frac{\partial p}{\partial y}+\Gamma\nabla^2 v+\frac{Ra}{Pr}T\sin\phi \tag{3}$$

$$u\frac{\partial T}{\partial x}+v\frac{\partial T}{\partial y}=\frac{k_r}{Pr}\nabla^2 T. \tag{4}$$

where Γ and k_r are both equal to one in the fluid region, and to 10^{15} and k_s/k_f, respectively, in the solid region.

The boundary conditions are as shown in Fig. 1 with a constant heat flux specified on the fin surfaces and the inner surface of the bounding massive wall.

$$\left.\begin{aligned} &u=v=0 \quad \text{on all solid walls}\\ &T=T_1 \text{ at } x=0,\quad 0\leqslant y\leqslant A\\ &T=0 \text{ at } x=1,\quad 0\leqslant y\leqslant A\\ &q=\text{constant} \quad \text{on the inner wall and fin surfaces}\\ &\frac{\partial T}{\partial y}=0 \text{ at } y=0, A \text{ and } 0\leqslant x\leqslant 1. \end{aligned}\right\} \tag{5}$$

$\Delta T'$ is known for a given Ra and ΔT is specified, which is used to determine the boundary condition at $x = 0$. Therefore, Ra and ΔT are the parameters specified for a solution.

At the bounding long sides, the local heat flux (or the local Nusselt number) and the average heat flux (or the average Nusselt number) are obtained, respectively, as

$$Nu_{loc}=\frac{hL'}{k_f}=\frac{1}{T_1}\frac{\partial T}{\partial x}\bigg|_{x=0,1} \tag{6}$$

$$Nu=\frac{\bar{h}L'}{k_f}=\frac{1}{AT_1}\int_0^A \frac{\partial T}{\partial x}\bigg|_{x=0.1} \mathrm{d}y. \tag{7}$$

The stream function is calculated from its definition and $\Psi = 0$ is assumed at the boundaries.

$$u=-\frac{\partial \Psi}{\partial y} \quad v=\frac{\partial \Psi}{\partial x}. \tag{8}$$

NUMERICAL METHOD

The numerical method used to solve the system of equations (1)–(4) with the boundary conditions of Fig. 1 and equation (5) is the SIMPLER method [7]. The computer code was validated for various cases and the results are published elsewhere [8]. The results for $Ra = 10^6$ showed that maximum deviations from the bench mark solutions [9] were $\Psi_{max} = 4.66\%$, $u_{max} = 3.34\%$, $v_{max} = 1.88\%$ and $Nu_0 = 6.81\%$.

A uniform grid size in both directions was used in this study with a minimum of three control volumes in solid media in the y direction. Independence of solution on the grid size was studied for various cases and k_r. For instance, for $Ra = 10^6$, $\phi = 90°$, $k_r = 20$, the grid size of 39×58 for the aspect ratio of $A = 2.5$, 39×118 for $A = 5$ and 39×178 for $A = 7.5$ was found to model accurately the flow and temperature fields. The results showed that grid independence was achieved above these grid sizes showing negligible

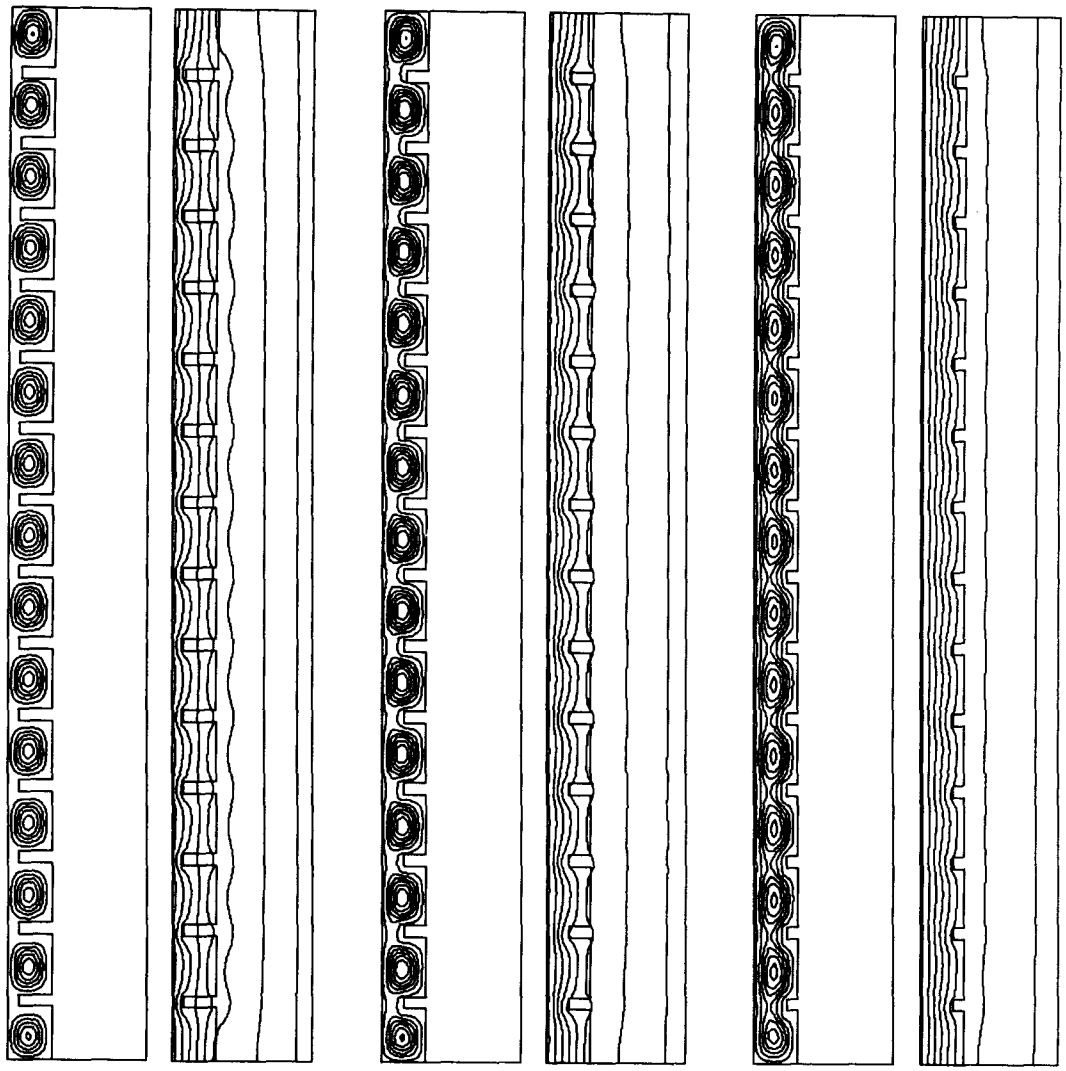

Fig. 2. Streamlines (on the left) and isotherms (on the right) for the case of $A = 7.5$, $C = 0.5$, $w = 0.66$, $\Delta T = 10$ K, $\phi = 90^\circ$, $k_r = 20$. (a) $B = 0.75$, $Ra = 10^6$, $\Psi_{ext} = 0.347$; (b) $B = 0.5$, $Ra = 10^6$, $\Psi_{ext} = 0.383$; (c) $B = 0.25$, $Ra = 10^6$, $\Psi_{ext} = 0.470$; (d) $B = 0.75$, $Ra = 10^8$, $\Psi_{ext} = 5.720, -0.100$; (e) $B = 0.5$, $Ra = 10^8$, $\Psi_{ext} = 5.950, -0.100$; (f) $B = 0.25$, $Ra = 10^8$, $\Psi_{ext} = 6.376, -0.030$.

differences in heat transfer (0.12%) and flow field, u, v (0.01%). The number of iterations was 150 for $A = 2.5$ and 320 for 7.5. For high Rayleigh numbers, the solution from lower Rayleigh numbers was used to initialize the computation so that the number of iterations was reduced considerably. The relaxation coefficient was from 0.8 for low Rayleigh numbers to 0.1 for high. For instance, for $Ra = 10^6$, $\phi = 90^\circ$, $k_r = 20$, using 39×58 grid size, the solution was obtained after 200 iterations requiring 70 min on an IBM RS/6000-365 workstation.

The convergence criteria were based on the corrected pressure field. When the correction terms were small enough so that no difference existed between the pressure field before and after correction, the computation was stopped. Hence,

$$\sum_{i=1}^{i_{max}} \sum_{j=1}^{j_{max}} b_{i,j} < 10^{-4} \tag{9}$$

where $b_{i,j}$ is the source term in the pressure correction equation.

The accuracy of computations was controlled also using the energy conservation within the system, which showed an accuracy within 0.1% in the worst case.

RESULTS AND DISCUSSION

The controlling geometrical parameters were as follows: $A = H'/L'$ was varied from 1 to 10, $B = l'/L'_1$ from 0 (system without fins) to 1 (enclosures with partitions), $C = h'/L'$ from 0.25 to 2.5, $w = w'/L'$

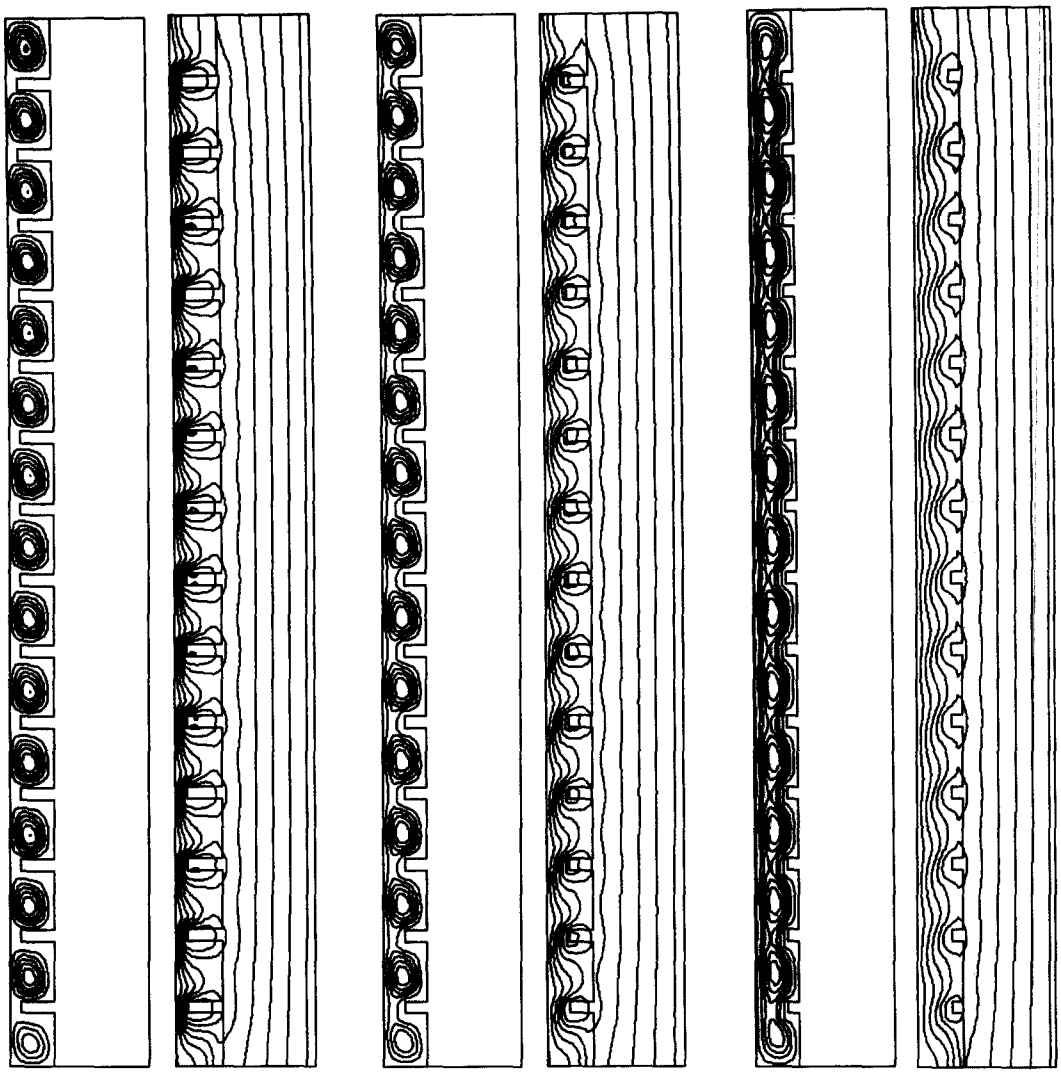

Fig. 2—*continued.*

from 0 to 1, the fin thickness was 0.08 and constant, and the inclination angle ϕ was from 5 to 90° (vertical system). Thermophysical parameters were $10^4 \leqslant Ra \leqslant 10^8$, $-50\,\text{K} \leqslant \Delta T = T_1' - T_2' \leqslant 50\,\text{K}$ and $10^{-3} \leqslant k_r \leqslant 10^5$. The range of the geometrical and thermophysical parameters and the variation of temperature difference cover practical situations. A base case was taken with $\phi = 90°$, $k_r = 20$, $A = 2.5$, $B = 0.75$, $C = 0.5$, $w = 0.66$, $\Delta T = \pm 10\,\text{K}$. The effects of A, B, C, w, k_r, ϕ were examined as required.

General observations

Streamlines and isotherms for the base case with $\Delta T = 10\,\text{K}$ are presented in Fig. 2(a)–(c) for $Ra = 10^6$, (d)–(f) for $Ra = 10^8$, each with $B = 0.75$, 0.5, 0.25. Isotherms on the right of each case in Fig. 2(a)–(c) show that, for $Ra = 10^6$, the heat transfer is dominated by conduction. For $B = 0.75$, a cell is formed in each micro-cavity, effectively cutting off any circulation along the left long side at $x = 0$. For $B = 0.50$ in Fig. 2(b), the fluid circulates along the left long side as well as through the micro-cavities. When B further decreased, Fig. 2(c) shows that the circulation in the enclosure is increased, although the cells in each micro-cavity are maintained. Ψ_{ext} values are -0.347, -0.383 and -0.470 for decreasing B, respectively, indicating that the circulations in the micro-cavities and in the enclosure are clockwise and their strengths increase with decreasing B. Isotherms in the solid wall show that temperature gradient increases with increasing B, an indication of higher heat transfer through the wall.

Figure 2(d)–(f) shows similar results for $Ra = 10^8$. Streamlines for higher Ra show similar appearance as for $Ra = 10^6$, although the strength of circulations increased considerably and their directions changed.

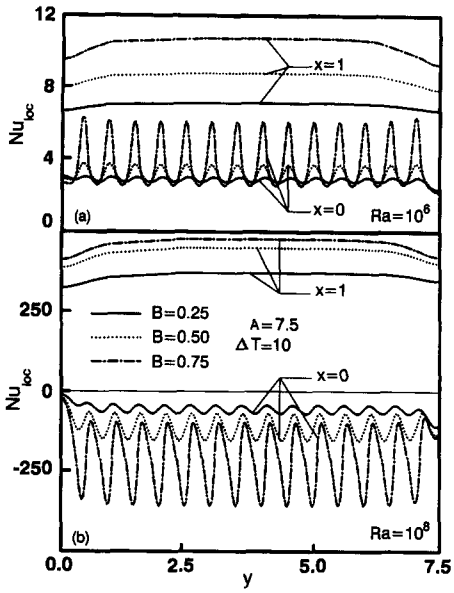

Fig. 3. Local Nusselt number at the bounding long sides $x = 0$ and 1 for various Ra and B. (a) $Ra = 10^6$, (b) $Ra = 10^8$. The other parameters are as in the base case.

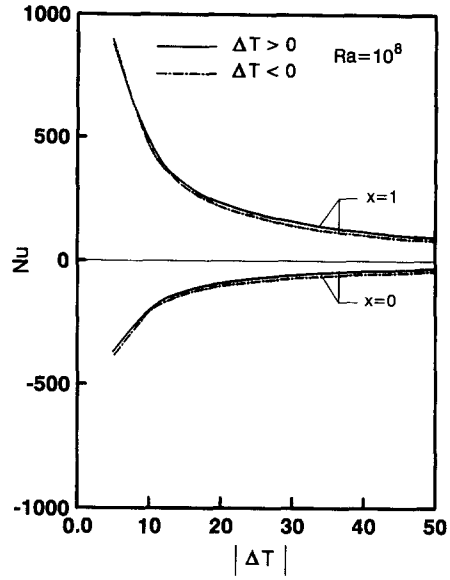

Fig. 4. Average Nusselt number as a function of temperature difference at the bounding long sides $x = 0$ and $x = 1$. The other parameters are as in the base case.

Ψ_{ext} values are 5.720, 5.950 and 6.376 for decreasing B, respectively, showing a counter clockwise rotation in the micro-cavities and in the enclosure. As expected, their strengths are increasing with decreasing B. Isotherms show that temperature gradient in the solid wall has increased with increasing Ra and decreased with decreasing B.

Reversing of the circulation direction of the cells in the micro-cavities and in the enclosure with increasing Rayleigh number is a consequence of the change of direction of heat flux through the left long side of the enclosure. Ψ_{ext} as a function of Ra and for various B were examined for the same case as Fig. 2. It was seen that Ψ_{ext} was negative up to 4.5×10^6, above which it became positive and increased sharply with increasing Ra. It was seen also that the variation of Ψ_{ext} below $Ra = 10^6$ down to 10^4 was negligibly small, an expected result since the heat transfer is dominated by conduction even at $Ra = 10^6$.

Heat transfer

Local heat transfer on the left long side at $x = 0$ and on the right at $x = 1$, is computed by equation (6) for $Ra = 10^6$ and 10^8 for various B. The results are presented in Fig. 3. Following the observations made for Fig. 2, the local Nusselt number is all positive for $Ra = 10^6$ at $x = 0$ and $x = 1$, i.e. the heat flows in the positive x direction through the two long sides. Nu_{loc} at $x = 1$ is generally higher than that at $x = 0$, since the former includes, in addition to the heat flowing from outside, the heat released by the solid wall and fins. At $x = 0$, the variation of Nu_{loc} is sinuous, the extremum of which corresponds to the fins. Their amplitude (also their average value) is increasing with increasing B, an expected result in view of the observations made earlier with Fig. 2. At $x = 1$, Nu_{loc} is more uniform along y and an increasing function of B. For $Ra = 10^8$, Nu_{loc} at $x = 0$ and 1 has different sign, i.e. the heat flow through the left long side is in the negative x direction, and therefore outwards on both sides. The heat released at the wall and fins are divided in two parts, the one to the left is transferred by convection, the other to the right by conduction through the wall. At high Ra, Nu_{loc} is still an increasing function of B. This is expected since the heat transfer surface increases with increasing B. The variation of Nu_{loc} is similar to the previous case with $Ra = 10^6$, quite uniform at $x = 1$ and sinuous at $x = 0$, for which similar observations can be made.

Average Nusselt number is calculated by equation (7) at $x = 0$ and 1 as a function of $|\Delta T|$ for $B = 0.75$ and $Ra = 10^8$, and presented in Fig. 4. The absolute value of Nu is a decreasing function of $|\Delta T|$ and there is a negligible difference between Nu with positive or negative ΔT. However, Nu is higher at $x = 0$ when $\Delta T < 0$ and it is so at $x = 1$ when positive. Nu at $x = 0$ is negative, i.e. the heat flow is in the negative x direction and its magnitude is lower than that at $x = 1$.

Average Nusselt number as a function of Ra for two aspect ratios is shown in Fig. 5, for various B and $\Delta T = 10$ K. It is seen that, at low Rayleigh numbers, the heat transfer being dominated by conduction is poor and the effect of the convection is evident when $Ra > 10^7$. Following earlier observations with negative and positive Nu at $x = 0$ and 1, heat transfer is from the enclosure outwards through the long sides. As expected, the absolute value of Nu is an increasing function of B.

Effect of aspect ratio A

The effect of the aspect ratio on the heat transfer was studied for the base case for A from 1 to 10.

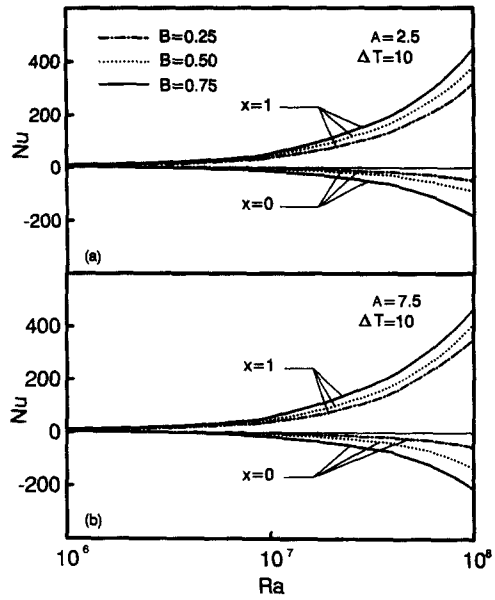

Fig. 5. Average Nusselt number as a function of Ra for various B and $\Delta T = 10$ K. (a) $A = 2.5$, (b) $A = 7.5$. The other parameters are as in the base case.

$Ra = 10^7$, 10^8, and $\Delta T = \pm 10$ K. It was seen that the effect of A was non-negligible only at high Ra and at low aspect ratios. From the heat transfer point of view, the enclosures with an aspect ratio greater than about 4 behave like one with $A \to \infty$.

Effect of fin length B

The effect of the dimensionless fin length on the heat transfer is studied for the base case for $A = 2.5$, $Ra = 10^6$–10^8, $\Delta T = \pm 10$ K and the results are presented in Fig. 6. Following the general observations

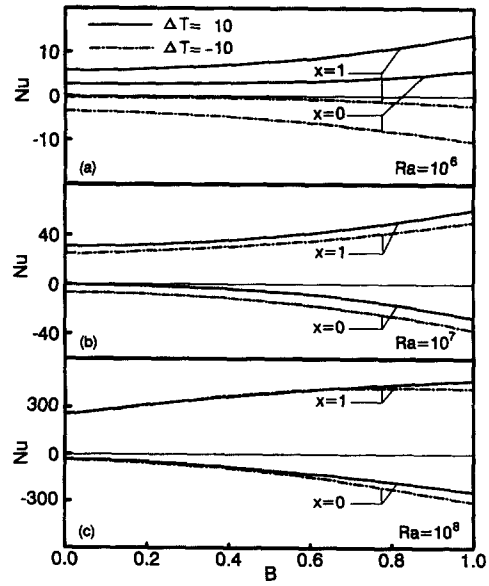

Fig. 6. Average Nusselt number as a function of the fin length at the long sides $x = 0$ and $x = 1$ for various Ra and ΔT. The other parameters are as in the base case.

made for Fig. 2, for $Ra = 10^6$ the heat transfer is in the positive x direction when $\Delta T = 10$ K and in the negative x direction when $\Delta T = -10$ K. The situation is different for $Ra = 10^7$ and 10^8, with Nu always positive at $x = 1$ and always negative at $x = 0$, since for high Ra numbers the convection dominates and the heat flow is from the enclosure outwards through the long side at $x = 0$. Generally, Nu is an increasing function of B since the heat transfer surface, and therefore the heat flow, increases with increasing B.

Effect of micro-cavity height C

Streamlines and isotherms for the base case with $A = 2.5$, $Ra = 10^8$ and $\Delta T = 10$ K for $C = 1.125$, 0.833, 0.5 and 0.25 are shown in Fig. 7. The corresponding number of micro-cavities is 2, 3, 5 and 10, respectively. Ψ_{ext} values are 6.12, 6.74, 5.79 and 1.23, all positive, indicating a counter-clockwise rotation, i.e. the heat transfer is from the enclosure to the left long side. Number of cells is identical to the number of micro-cavities, n for cases (a)–(c), without any interaction among them. In case (d), double cells are formed in each micro-cavity, except at the bottom and top. In all cases there is no circulation through the enclosure since it is cut off effectively by rotating cells at each micro-cavity. Isotherms show increasing temperature gradient in the enclosure and through the solid wall with decreasing C. Thus the heat transfer is more favorable for decreasing C.

Average heat transfer at $x = 0$ and 1 as a function of C is shown in Fig. 8 for $Ra = 10^7$, 10^8 and $\Delta T = \pm 10$ K, the other parameters being identical with the base case. Following the observations made for Fig. 7, the variation of Nu is most pronounced for small C. The heat transfer for both Ra is outwards through the long sides. As Ra increases, the difference in Nu for positive or negative ΔT decreases.

Effect of wall thickness w

Streamlines and isotherms for the base case with $A = 7.5$, $Ra = 10^8$ and $\Delta T = 10$ K and $w = 0.051$, 0.359 and 0.769 are shown in Fig. 9. The case with $w = 0.66$ is presented in Fig. 2(d). Streamlines show double cells in micro-cavities when w is relatively small as in Fig. 9(a) and (b). The strength of double cells in Fig. 9(a) for $w = 0.051$ has the same order of magnitude with $\Psi_{ext} = +16.796$, -11.974. The cells with negative value are those inside the micro-cavities rotating clockwise and those with positive value are near the left long side rotating counter-clockwise. It is seen that these cells are interconnected with a strong circulation in the enclosure. As w increases to 0.359, the strength of inner cells is reduced and they are no longer visible for $w = 0.66$ in Fig. 2(d) and 0.769 in Fig. 9(c), although they exist as evidenced by the negative values of Ψ_{ext} of -0.1 and -0.042, respectively. These observations are indications that the heat transfer at $x = 0$ is in the negative x direction, i.e. from enclosure outwards. Isotherms for the same cases support the previous observations on stream-

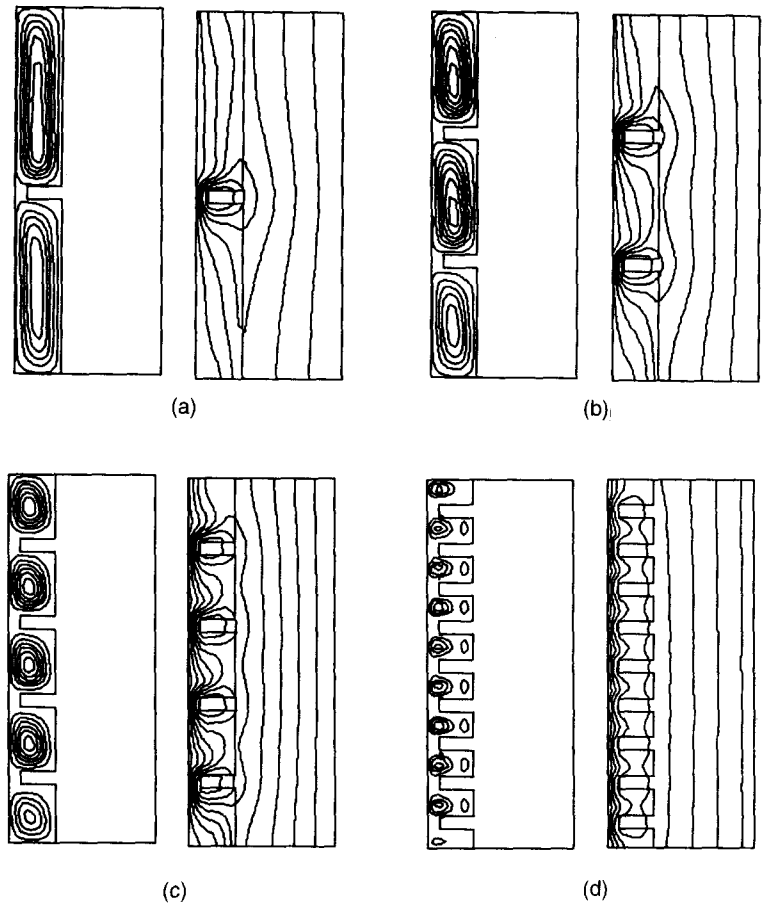

Fig. 7. Streamlines (on the left) and isotherms (on the right) for the case with $A = 2.5$, $B = 0.75$, $\Delta T = 10$ K, $\phi = 90°$, $k_r = 20$ and $Ra = 10^8$. (a) $C = 1.125$, $\Psi_{ext} = 6.120, -0.030$; (b) $C = 0.833$, $\Psi_{ext} = 6.740, -0.031$; (c) $C = 0.5$, $\Psi_{ext} = 5.790, -0.085$; (d) $C = 0.25$, $\Psi_{ext} = 1.226, -0.100$.

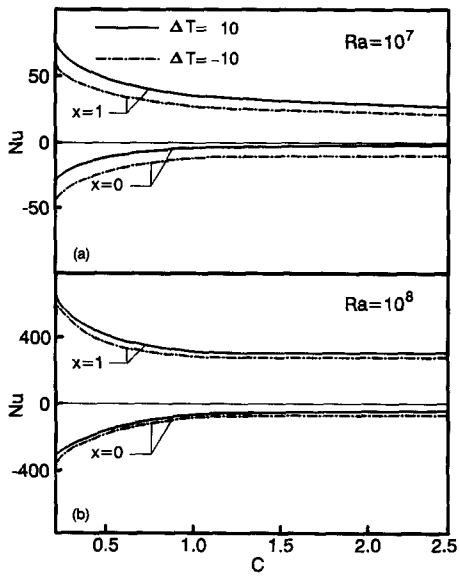

Fig. 8. Average Nusselt number as a function of C for the same case of Fig. 11 with $\Delta T = \pm 10$ K. (a) $Ra = 10^7$, (b) $Ra = 10^8$. The other parameters are as in the base case.

lines. As w increases, the heat transfer becomes more dominated by conduction, an indication of lower heat transfer at $x = 1$ with increasing w.

Average heat transfer at $x = 0$ and 1 is calculated for the same case with $Ra = 10^8$ and $\Delta T = \pm 10$ K as a function of w and the results are presented in Fig. 10. As discussed earlier, for high Ra numbers, the heat transfer is outwards at both long sides: therefore, the heat transfer at $x = 0$ is negative. It is seen that, as the wall thickness increases, Nu decreases through the right long side, since the resistance is higher for thicker wall. The decrease of the $|Nu|$ at $x = 0$ is small, which is explained by the reduced convection as noted in Fig. 9. Nu at $x = 1$ is slightly higher for $\Delta T = 10$ K than -10 and the reverse is true for Nu at $x = 0$, an expected result in view of the findings in Fig. 4.

Effect of conductivity ratio k_r

Streamlines and isotherms for the base case with $A = 2.5$, $Ra = 10^8$, $\Delta T = 10$ K and $k_r = 0.01$, 1, 10^5 are shown in Fig. 11. The case with $k_r = 20$ is presented in Fig. 7(c). Streamlines show that, for increas-

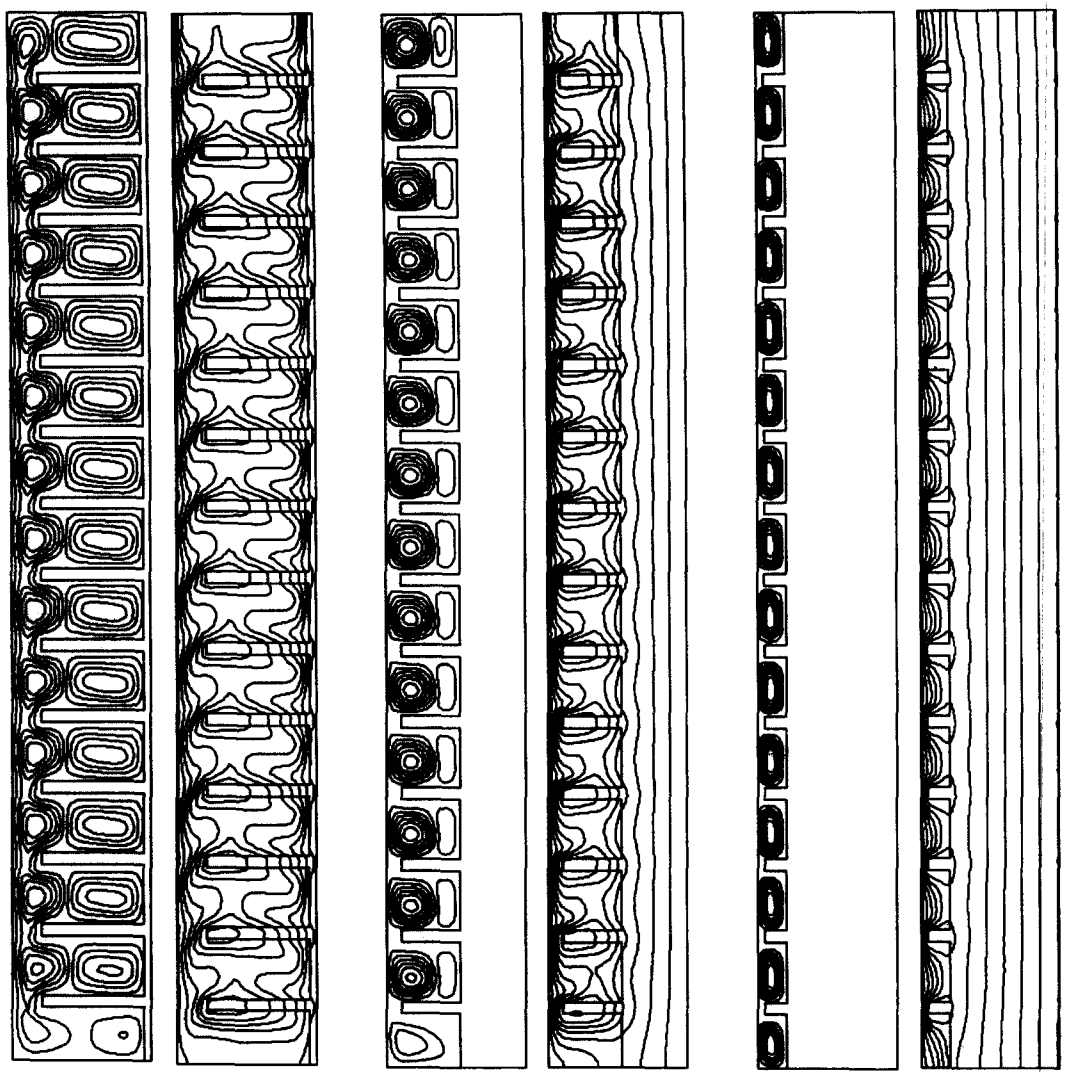

Fig. 9. Streamlines (on the left) and isotherms (on the right) for the case with $A = 7.5$, $B = 0.75$, $C = 0.5$, $\Delta T = 10$ K, $\phi = 90°$, $k_r = 20$ and $Ra = 10^8$. (a) $w = 0.051$, $\Psi_{ext} = 16.796$, -11.974; (b) $w = 0.359$, $\Psi_{ext} = 9.600$, -2.783; (c) $w = 0.769$, $\Psi_{ext} = 2.033$, -0.042.

ing k_r, Ψ_{ext} decreases, an indication of reduced convection and increasing conduction. The cells formed in each micro-cavity rotate in a counter-clockwise direction for $k_r = 10^{-2}$, 1, 20 and clockwise for 10^5. This indicates that the heat transfer for the former cases is outwards at $x = 0$, and inwards for the last case. Isotherms show the supporting evidence for these observations: the heat transfer by conduction is seen to increase with increasing k_r.

Average heat transfer for the same case is plotted in Fig. 12 with $\Delta T = \pm 10$ K and $Ra = 10^7$ and 10^8. Confirming the observations made in Fig. 11, Nu at $x = 1$ is an increasing function of k_r and $|Nu|$ at $x = 0$ is high at low k_r, decreasing until zero and then changing sign from negative to positive. This trend is more pronounced when $Ra = 10^7$. Similar observations can be made on the effect of ΔT as for Figs. 8 and 10 following Fig. 4. It is noted that, for very small k_r, the heat transfer at $x = 1$ is zero or negligibly small, since this case corresponds to insulating walls.

Effect of inclination angle ϕ

Average Nusselt numbers were calculated corresponding to the base case and with $A = 2.5$, $Ra = 10^8$, $\Delta T = \pm 10$ K as a function of the inclination angle. It was seen that $|Nu|$ was a decreasing function of ϕ at $x = 1$ and an increasing function at $x = 0$. The relative variations were from 5 to 20%. Streamlines and isotherms were produced for various ϕ, as in Fig. 7(c) for $\phi = 90°$, which were all similar for near-vertical angles, with a single convection cell rotating in a counter-clockwise direction in each micro-cavity. At low angles, the counter-clockwise rotating cell was accompanied by a clockwise rotating cell, except at the lowest micro-cavity. The isotherms

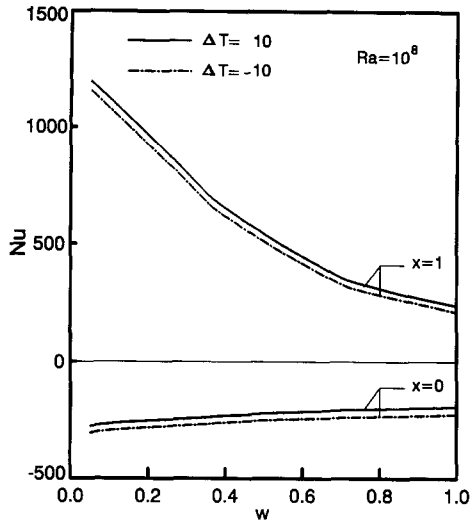

Fig. 10. Average Nusselt number at $x = 0$ and 1 as a function of the wall thickness for the same case as Fig. 9 with $\Delta T = \pm 10$ K, $Ra = 10^8$. The other parameters are as in the base case.

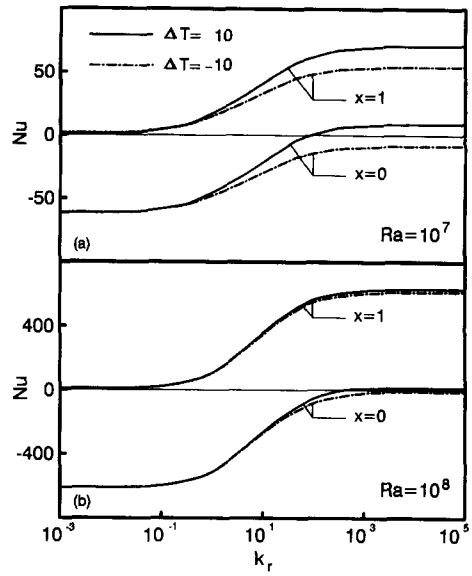

Fig. 12. Average Nusselt number at $x = 0$ and 1 as a function of the wall conductivity ratio for the same case as Fig. 11 with $\Delta T = \pm 10$ K, $Ra = 10^8$. The other parameters are as in the base case.

were almost identical, an indication of a small effect on heat transfer.

CONCLUSIONS

The following conclusions are drawn:

(1) It is found that heat transfer from the inner surface of the wall and fins through the two bounding long sides is dominated by conduction at low Rayleigh numbers and by convection at high numbers. The heat flow at low Rayleigh numbers is inwards through the left long side with zero thickness, which may have different consequences for different applications. For instance, it will be undesirable in cooling of electronic components, but desirable in building components. At high Rayleigh numbers, the heat flow is outwards, making the cooling process an effective one.

(2) The effect of temperature difference on the heat transfer is high when $\Delta T < 20$ K, above which it is negligible. The heat transfer is an increasing function of the fin length, and of the enclosure aspect ratio, particularly at low aspect ratios, and a decreasing function of the micro-cavity aspect ratio and the wall thickness, particularly at their low values.

(3) The heat transfer is by convection through the left long side for low wall conductivities and through the right long side for high conductivities.

(4) The effect of the inclination angle on the heat transfer is small for ϕ from 5 to 90° (vertical position).

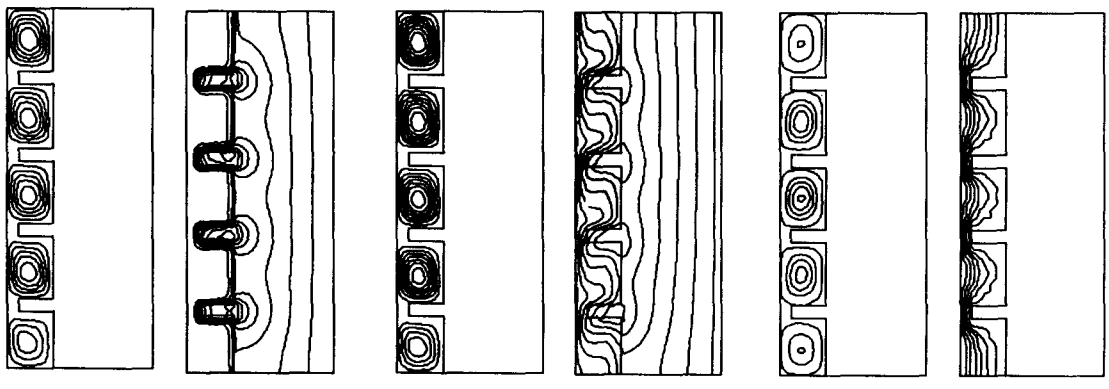

Fig. 11. Streamlines (on the left) and isotherms (on the right) for the case with $A = 2.5$, $B = 0.75$, $C = 0.5$, $\Delta T = 10$ K, $\phi = 90°$, $k_r = 20$ and $Ra = 10^8$. (a) $k_r = 0.01$, $\Psi_{ext} = 11.158$; (b) $k_r = 1$, $\Psi_{ext} = 5.790, -0.085$; (c) $k_r = 10^5$, $\Psi_{ext} = -1.059$.

Acknowledgements—Financial supports by Natural Sciences and Engineering Research Council of Canada, the FCAR of Quebec Province and Canadian International Development Agency (for the fellowship to E.K.L.) are acknowledged.

REFERENCES

1. Z. Zrikem and E. Bilgen, Theoretical study of a non-convective Trombe wall collector with honeycomb structure, *Solar Wind Technol.* **3,** 33–44 (1986).
2. M. Hasnaoui, Z. Zrikem, P. Vasseur and E. Bilgen, Radiation induced natural convection in enclosures with conducting walls, *Solar Wind Technol.* **7,** 515–525 (1990).
3. M. Hasnaoui, P. Vasseur and E. Bilgen, Natural convection in rectangular enclosures with fins attached to one of the isothermal walls. In *ASME Solar Engineering* (Edited by J. T. Beard and M. A. Ebadian), pp. 131–137. ASME, New York (1990).
4. M. Hasnaoui, P. Vasseur and E. Bilgen, Natural convection in rectangular enclosures with adiabatic fins attached on the heated wall, *Wärme- und Stoffübertragung* **27,** 357–368 (1992).
5. R. Scozia and R. L. Frederick, Natural convection in slender cavities with multiple fins attached to an active wall, *Numer. Heat Transfer* **20,** Pt A, 127–158 (1991).
6. E. K. Lakhal, M. Hasnaoui, E. Bilgen and P. Vasseur, Natural convection in inclined rectangular enclosures with perfectly conducting fins attached on the heated wall, submitted to *Appl. Res. Sci.*
7. S. V. Patankar, *Numerical Heat Transfer and Fluid Flow.* Hemisphere, Washington, DC (1980).
8. R. Ben Yedder and E. Bilgen, Natural convection and conduction in Trombe wall systems, *Int. J. Heat Mass Transfer* **34,** 1237–1248 (1991).
9. G. De Vahl Davis and I. P. Jones, Natural convection in a square cavity: a comparison exercise, *Int. J. Numer. Meth. Fluids* **3,** 227–248 (1983).